IBRO Neuroscience Reports 13 (2022) 410–419

Contents lists available at ScienceDirect

IBRO Neuroscience Reports

journal homepage: www.sciencedirect.com/journal/IBRO-Neuroscience-Reports

Pyruvate dehydrogenase kinase 1 promotes neuronal apoptosis upon Japanese encephalitis virus infection

Surajit Chakraborty, Ellora Sen, Anirban Basu *

National Brain Research Centre, Manesar, Haryana, India

A B S T R A C T

Infection by Japanese Encephalitis Virus (JEV) in humans is primarily characterized by signs and symptoms including non-specific febrile illness, arthralgia, myalgia etc. followed by its resolution due to joint action of host innate and adaptive immunity. However, in selective cases, complications arise owing to invasion of central nervous system (CNS) by JEV. Patients being unable to control peripheral viral replication owing to differences in host genetics and immunity experience JEV-associated neurological complications manifested in the form of headache, nausea, meningoencephalitis, coma and eventual death. Entry of JEV into CNS activates complex cascade of events resulting in loss of neuronal physiology and thus CNS tissue integrity. In present study, we have demonstrated role played by JEV in modulation of neuronal pyruvate dehydrogenase kinase 1 (PDK1) abundance and its effect upon neuronal health. Infection of neuron by JEV culminates into upregulation of PDK1 abundance. Albeit inhibition of JEV-induced PDK1-upregulation was accompanied by enhanced JEV propagation in neurons, abrogation of PDK1-upregulation was demonstrated to ameliorate neuronal apoptosis. PDK1 inhibition-associated reduction in neuronal death was observed to be associated with reduced generation of reactive oxygen species (ROS) in neurons. Our study hence provides a possible therapeutic target which upon modulation might help combat JEV infection-associated neuronal apoptosis via restoration of JEV-associated ROS generation.

1. Introduction

JEV belonging to family *Flaviviridae* and is a positive-sense single-stranded RNA virus found circulating predominantly in South-eastern Asia (Neufeldt et al., 2018). Infection by JEV is primarily characterized by signs and symptoms ranging from pyrexia, muscle pain, joint pain, coryza, diarrhea etc. However, JEV upon infecting infants and elderly might result into neurological complications manifesting as headache, nausea, Brudzinski's sign, encephalitis, coma eventually resulting into death of patient (Solomon et al., 2000). Histological examination of autopsy brain tissue harvested from deceased patients suffering from JEV-induced encephalitis demonstrates both diffuse and focal damage to CNS parenchyma (Johnson et al., 1985). Post-mortem findings from human brain tissue and analysis of brain tissue from primate model for JEV infection (Saw et al., 1999) point towards role of neuronal damage as contributing factor to neurological manifestations associated with JEV-induced encephalitis.

Neurons have been demonstrated to act as primary target for JEV infection supporting replication of the latter. Multiple reports point towards the role uncontrolled neuroinflammation in promoting neuronal apoptosis in the context of CNS invasion by JEV (Chambers and Diamond, 2003; Turtle and Solomon, 2018). Modulation of multiple apoptosis-promoting signaling pathways including intricate network of bcl-2 family of proteins by flaviviral infection culminate into activation of apoptotic machinery hence resulting into cell death (Suzuki et al., 2018; Tsao et al., 2008). Prolonged activation of endoplasmic reticulum stress (ER stress) pathway in host cell upon flaviviral infection has been demonstrated to lead to cell-death (Huang et al., 2016; Medigeshi et al., 2007; Wang et al., 2019). Understanding the mechanistic basis for activation of cell-death machinery thus holds significant promise in amelioration of host cell death-associated disease morbidity in cases of viral infection.

Viruses utilize host cell machinery for synthesis of biomolecules required for virus replication. Viruses upon infecting cells modulate host-cell metabolism to reshape host metabolic landscape in favor of viral replication (Sanchez and Lagunoff, 2015). Virus-induced alterations in lipid biosynthesis aid in change of lipid composition of intracellular or cell-surface membranes (Leier et al., 2018). These changes induced in host membranes help assembly of host and viral protein molecules thus providing a scaffold for successful virus genome

Abbreviations: JEV, Japanese Encephalitis Virus; CNS, central nervous system; PDK1, pyruvate dehydrogenase kinase 1; ROS, reactive oxygen species; Bcl-2, B-cell lymphoma 2; ER-stress, endoplasmic reticulum stress; JNK, c-Jun N-terminal Kinase; PDH, pyruvate dehydrogenase; WNV, West Nile virus; DCFDA, 5-(and-6)-chlromethyl-2′, 7′-dichlorodihydrofluorescein Diacetate; ATP, adenosine triphosphate; PERK, Protein Kinase RNA-like ER Kinase; CHOP, C/EBP Homologous protein.

* Corresponding author.
E-mail address: anirban@nbrc.ac.in (A. Basu).

https://doi.org/10.1016/j.ibneur.2022.10.011
Received 26 September 2022; Received in revised form 14 October 2022; Accepted 27 October 2022
Available online 29 October 2022

replication. Moreover, changes in membrane lipid composition (cell surface/intracellular) help shape the molecular nature of viral envelop thus helping in viral maturation process. In addition to lipid metabolism, viruses have been observed to alter nucleotide metabolism to provide nucleotide molecules required for viral genome replication (Sanchez and Lagunoff, 2015). Preference for/activity of metabolic pathways responsible for oxidation of glucose molecule has also been shown to be altered in the context of viral infections. Infection of cells by Dengue virus (Fontaine et al., 2015), Zika virus (Rothan et al., 2019) has been shown to be accompanied by increase in carbon flux via glycolysis pathway. SARS-CoV 2 (severe acute respiratory syndrome-Coronavirus 2) infection of monocytes has been observed to induce increase in glycolytic pathway activity (Bhatt et al., 2022). Inhibition of virus-mediated increase in glycolytic flux has been shown to be accompanied by reduction in infectious virus production thus underscoring the significance of infection-associated changes in host metabolism. Although changes in glucose metabolism pathways have implications in terms of energy production, reactive oxygen species (ROS) generation also gets significantly affected depending upon the choice of glucose oxidation pathway being operational in host cell. Given the established role of ROS in inducing cytotoxicity in the context of flavivirus infection (Zhang et al., 2019), deciphering molecular mechanism responsible for regulating ROS generation in neurons upon viral infection holds significant promise to combat infection-induced neuronal death thus combating neurological manifestations associated with JEV infection.

With these findings in mind, we attempted to assess the mechanistic basis for regulation of ROS generation in neurons upon JEV infection. JNK phosphorylation has been demonstrated to play crucial role in JEV-induced neuronal apoptosis (Chakraborty and Basu, 2022; Huang et al., 2016). Since JNK activation is reported to inhibit pyruvate dehydrogenase (PDH) complex (as a result of phosphorylation) thus reducing metabolic flux of glucose oxidation from glycolysis to TCA cycle, and PDH complex acts as a primary substrate for pyruvate dehydrogenase kinase (PDK) (Wang et al., 2021), we evaluated the effect of JEV infection upon PDK-1 abundance in neurons upon JEV infection. Our study highlights a previously unknown role of PDK1 in the generation of ROS crucial for neuronal fate upon JEV infection.

2. Methods

2.1. Mice

Neonatal BALB/c mice (irrespective of sex) were harbored with their respective mothers under conditions of constant temperature and humidity. Animals were maintained in 12-hour day- and 12-hour night-cycle with the motive of not disrupting their normal circadian rhythm. Animals used during experiments and maintenance were handled with utmost care as per recommendations mentioned in protocols issued by Committee for the Purpose of Control and Supervision of Experiments on Animals, Ministry of Environment and Forestry, Government of India. All the experiments were approved by Animal Ethics Committee of National Brain Research Centre (NBRC/IAEC/2017/30).

2.2. Cell-culture

Human neuroblastoma cell-line SH-SY5Y was procured (as a kind gift) from Dr. S Levison, Rutgers University, School of medicine, New Jersey. SH-SY5Y cells were maintained using Dulbecco's minimal essential media: F12 (DMEM: F12, Gibco) supplemented with 10 % FBS (Gibco) and 10 % penicillin-streptomycin (Invitrogen,100 μg/ml). Porcine kidney cells (PS-cells) and Vero-E6 cells were also maintained using DMEM (Gibco) containing 10 % FBS (Gibco) and 10 % penicillin-streptomycin (Invitrogen,100 μg/ml). Cell-cultures were maintained in a humidified cell-culture incubator at 37 °C, 5 % CO_2.

2.3. Virus propagation and measurement of viral titer

2-day old BALB/c mice were employed for propagation of Japanese encephalitis and West Nile virus (WNV). Neonatal mice pups were housed with their respective mothers. On day 2 post-partum, pups were infected with 5000 particles of JEV and WNV using intracranial route. Following infection, neonatal mice were kept under observation (housed with respective mothers) and assessed for appearance of signs of infection. Following 5–6 days of infection, mice-pups presented with severe signs of infection and were euthanised for collection of brain tissue. Brain samples were collected in sterile PBS followed by homogenization to generate homogeneous suspension. Mouse brain homogenate was centrifuged at 4 °C, 15,000 revolutions per minute (rpm) for 45 min. Following centrifugation, supernatant obtained was collected and pellet containing tissue debris was discarded. Supernatant containing virus particles was filtered using 22 μm filter to remove any remnant tissue debris from the supernatant. The filtrate was stored at minus 80 °C for further experimentation. Filtrate obtained was also used for measurement of viral titer. Porcine kidney cells (PS cells) and Vero-E6 cells were utilized to measure number of infectious JEV and WNV particles respectively. In brief, PS/Vero-E6 cells were cultured in monolayer. Cell monolayers were serum-starved for 2 h prior to incubation with different dilutions of viral particles. Following incubation with virus dilutions, cells were thoroughly washed with PBS to remove any remaining loosely adsorbed viral particles. Cells were then covered with low-melting agarose overlay containing cell-culture media (MEM, Gibco) and fetal bovine serum (Gibco) and incubated at 37 °C for 96 and 72 h (for estimation of JEV and WNV titer respectively). Agarose overlay was then removed followed by staining of cells with crystal violet solution (Sigma) for visualization of plaques.

2.4. Esi-RNA transfection of SH-SY5Y cells using lipid-based transfection reagent

SH-SY5Y cells were transfected with esi-RNA specific for human pyruvate dehydrogenase kinase 1 (esi-RNA-human-PDK1, Sigma-Aldrich, USA, cat. no.: EHU-079981–20UG) or EGFP-specific esiRNA (Sigma-Aldrich, USA, cat. no.: EHUEGFP-50UG) using lipid-based transfection reagent Lipofectamine 2000 (Invitrogen) and Opti-MEM (Gibco) as per recommendations by manufacturer. In brief, cells were serum-starved for 2 h prior to incubation with esi-RNA and lipofectamine 2000 for 8 h. Cells were then washed thoroughly with PBS to remove excess esi-RNA and transfectant solution followed by maintenance in cell-culture media (DMEM: F12, supplemented with FBS and Penicillin-streptomycin) for another 16 h. Mock-transfection (MT) was performed by incubating cells in Opti-MEM with Lipofectamine-2000 without any nucleic-acid for 8 h followed by further maintenance for 16 h. Upon completion of transfection, cells were then treated as indicated in the experiments.

2.5. Infection of SH-SY5Y cells by JEV and WNV

In brief, SH-SY5Y cells maintained in DMEM: F12 supplemented with 10 % FBS (Gibco) and 10 % Penicillin-streptomycin (Invitrogen,100 μg/ml) were serum-starved for 2 h prior to incubation with viruses. Following serum starvation, JEV (Gp78-strain) and WNV (Eg-101-strain, procured from National Institute of Virology, Pune, India) were added to cultured cells at multiplicity of infection (MOI) 3 for 2 h. Cells were then washed thoroughly with filtered PBS solution to remove the excess loosely adsorbed viral particles. SH-SY5Y cells were then incubated for time periods as indicated in the experiment prior to collection for further processing.

2.6. Polymerase chain reaction

Cells undergoing treatment under diverse conditions as indicated in

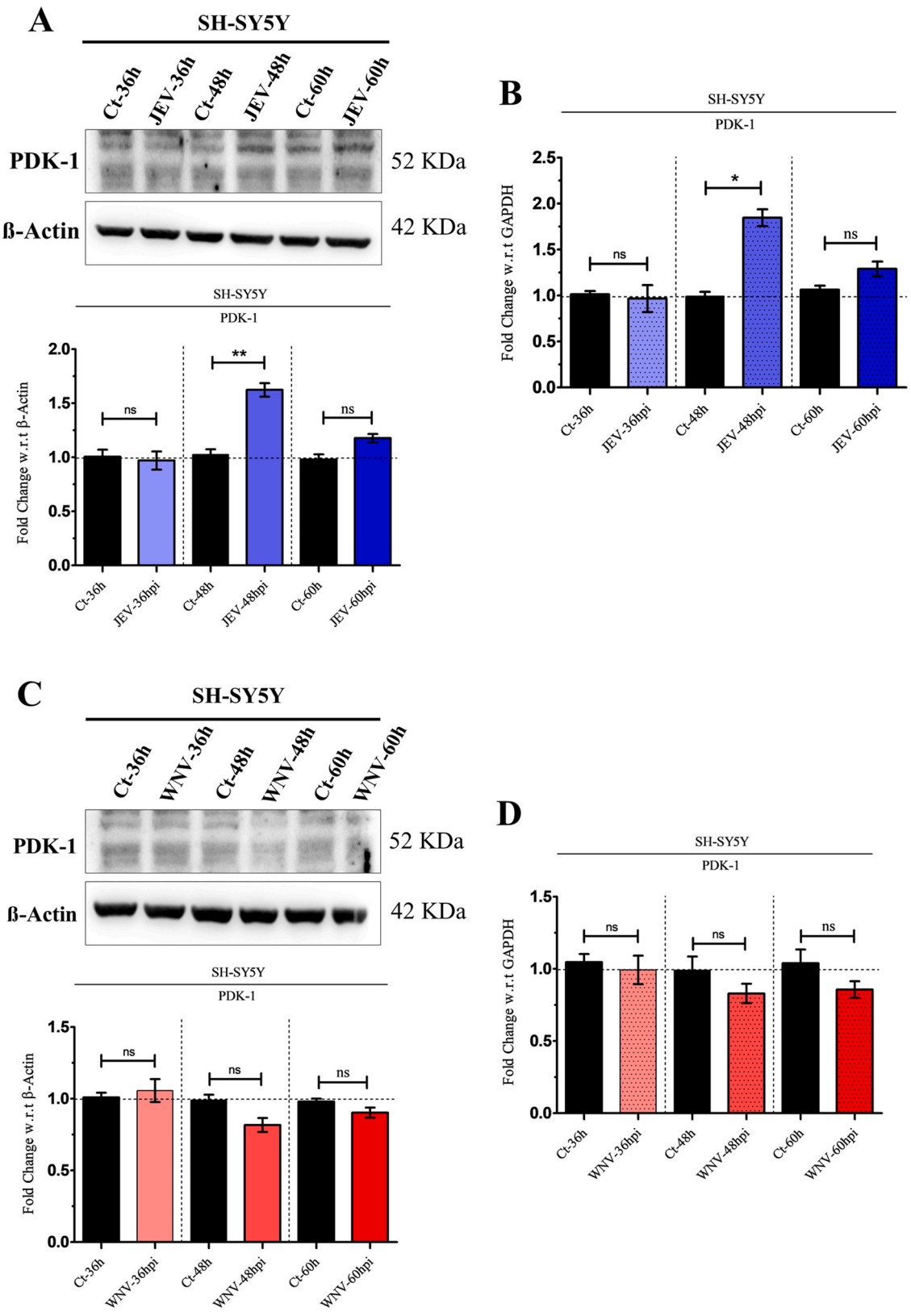

Fig. 1. JEV induces PDK-1 upregulation in SH-SY5Y cells. SH-SY5Y cells subjected to infection by JEV (A, quantitative analysis: A bottom) and WNV (C, quantitative analysis: C bottom) at multiplicity of infection (MOI) 3 were harvested after respective time periods (36, 48 and 60 hpi) and were utilized for protein isolation for estimation of PDK-1 abundance. ß-Actin abundance was used as loading control. RNA isolated from SH-SY5Y cells infected with JEV (B) and WNV (D) at MOI 3 for 36, 48 and 60 hpi were subjected to RNA isolation. RNA was converted to cDNA followed by qRT-PCR for estimation of PDK-1 transcript abundance. GAPDH was used as loading control. Graphs provided in the figure represent data in the form of mean ± SD from three independent experiments with similar outcome. *P < 0.05, **P < 0.01 and ns: non-significant, by two-tailed student's t-test.

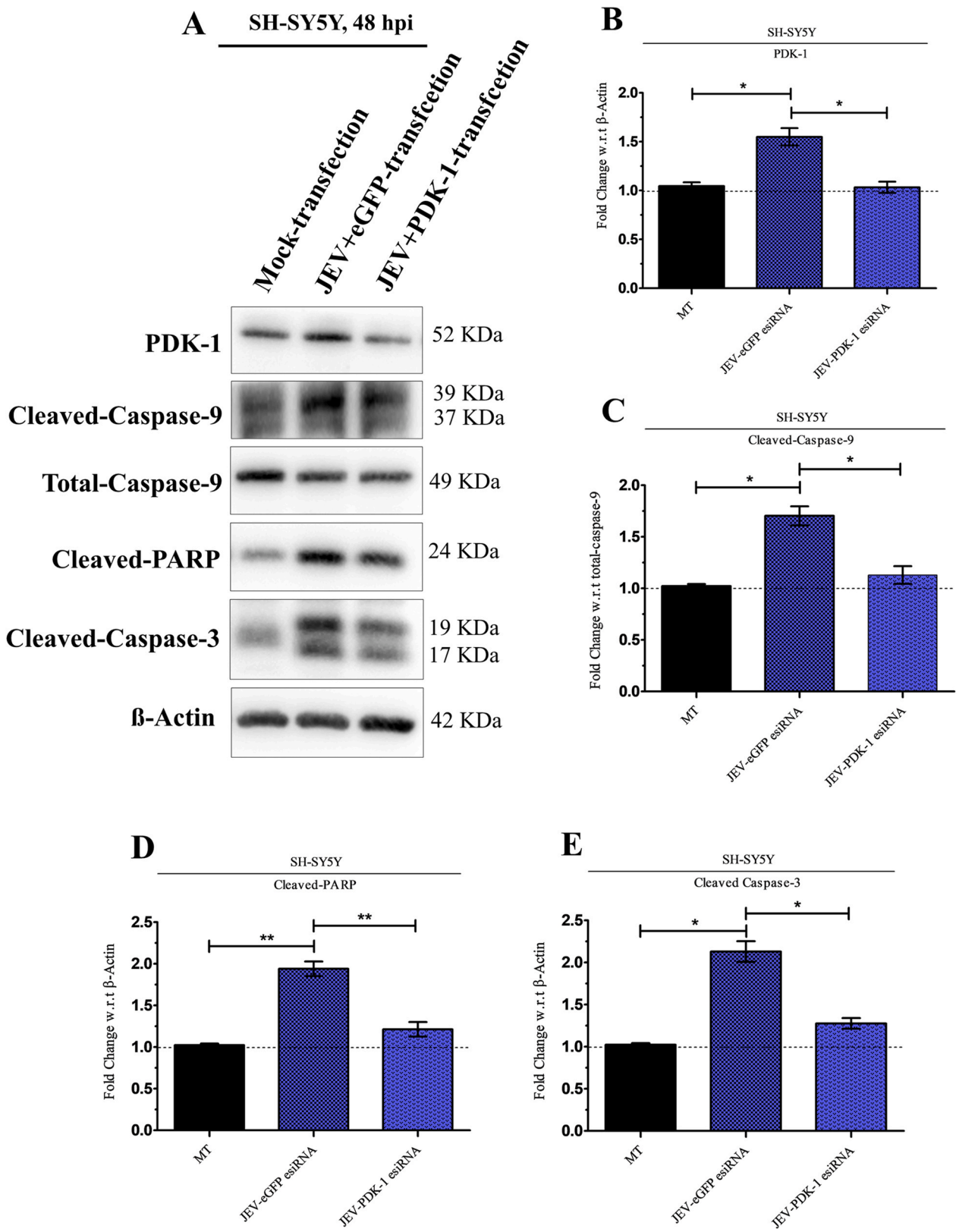

Fig. 2. PDK-1 upregulation in JEV-infected SH-SY5Y cells promotes neuronal apoptosis. Protein was isolated from SH-SY5Y cells (uninfected + mock-transfected, JEV-infected + enhanced GFP-transfected and JEV-infected + PDK-1 esiRNA-transfected cells). Infection was performed at 3 MOI for 48 h post infection. Protein was subjected to immunoblotting experiment for estimation of PDK-1, cleaved caspase-9, total caspase-9, cleaved-PARP and cleaved caspase-3 abundance (A). ß-Actin was used as loading control. Quantitative analysis of Western blotting experiments demonstrates expression level of PDK-1 (B, with respect to ß-Actin), cleaved caspase-9 (C, with respect to total caspase-9), cleaved-PARP (D, with respect to ß-Actin) and cleaved caspase-3 (E, with respect to ß-Actin) abundance under different conditions. Bar graphs provided in the figure represent data in the form of mean ± SD from three independent experiments exhibiting similar outcome. Statistical significance of difference in values between two groups has been estimated using two-tailed Student's t-test. *$P < 0.05$, **$P < 0.01$.

figures were harvested at time-points as indicated by experiments. Following collection of cell samples, RNA was isolated using phenol-chloroform method. In brief, cells were treated with Trizol (Sigma) followed by addition of chloroform (Merck). Upon separation of different phases as a result of centrifugation, the clear phase (containing RNA molecules) was collected. The clear solution was treated with isopropanol (Merck) for precipitation of RNA prior to washing with 75 % ethyl alcohol (Merck). Concentration of RNA was estimated using spectrophotometer (Thermo Scientific, Varioskan Sky) and used for conversion into complementary DNA (cDNA) molecules using kit (Thermo Verso cDNA synthesis kit) as per manufacturer's instruction. Equal amount (in nanograms) of RNA molecules was used across multiple samples for cDNA preparation. cDNA was then used for quantitative real-time polymerase chain reaction (qRT-PCR) using SYBR-Green (Applied Biosystems) or semi-quantitative PCR (followed by PCR product electrophoresis in agarose gel) using Taq polymerase enzyme, nucleotide mix, Taq polymerase buffer from New England Biolabs (NEB) for relative estimation of JEV-GP78, tm: 54 ºC, (Forward primer: CAGGGAAGAGATCAGCCATTAG, Reverse primer: GGAGCATGTACC-CATAGTGAAG), human PDK-1, tm: 45 ºC, (Forward primer: ATCAC-CAGGACAGCCAATAC, Reverse primer: CCTCGGTCACTCATCTTCAC), human hexokinase-2, tm: 62 ºC, (Forward primer: TCGCATCTGCTTGCCTACTTC, Reverse primer: CTTCTGGAGCC-CATTGTCCGT) transcript abundance. Human GAPDH abundance, tm: 55 ºC, was estimated for its use as loading-control (Forward primer: GCAAATTCCATGGCACCGT, Reverse primer: TCGCCCCACTGATT TTGG).

2.7. Western blotting

Cells undergoing treatment with different conditions were harvested for isolation of proteins. Buffer containing 10 mM tris-HCl (pH 8.0), 1 % Triton X-100, 150 mM NaCl, 0.5 % NP-40, 1 mM EDTA, 0.2 % EGTA, 0.2 % sodium orthovanadate, and protease-inhibitor cocktail (Sigma Aldrich, USA) was used to lyse the cells. Following lysis, the cell lysate was subjected to sonication for increasing protein yield. Following sonication, the solution was centrifuged at 12,000 rpm for 30 min (at 4 ºC). Supernatant containing protein was collected and pellet containing cellular debris from lysis was discarded. Concentration of protein was estimated using bicinchoninic acid- (BCA) method. Proteins were then loaded onto sodium-dodecyl sulfate (SDS, Sigma)-polyacrylamide (containing acrylamide and bisacrylamide, Sigma) gel and electrophoresed to separate them on the basis of their molecular weight. Upon completion of electrophoresis, proteins were transferred to nitrocellulose membrane (GE technologies). Membranes containing proteins were blocked using fat-free milk solution (Himedia) at room-temperature. Following incubation with blocking-solution, blots were probed for protein molecules by incubating with primary antibodies specific for respective proteins at 4 ºC for 12 h: human PDK-1 (1:1000, Novus Biologicals) ß-actin (1:10,000 Sigma Aldrich), cleaved-PARP (1:1000, Abcam), caspase-9 (1:1000, Cell Signaling Technology), JEV-NS3 (1:10000, Gentex) and cleaved caspase-3 (1:1000, Cell Signaling Technology). Primary antibody-bound membranes were then washed thoroughly using Tris-buffered saline solution containing Tween-20 detergent (TBST solution) for removal of unbound primary antibodies. Blots were then incubated with peroxidase-labeled anti-rabbit or anti-mouse secondary antibodies (1:2000, Cell Signaling Technology) at room-temperature followed by washing using TBST solution to remove loosely-bound secondary antibodies. Chemiluminescence from the nitrocellulose membranes was measured using Chemigenius bioimaging system (Uvitec Cambrige, Cleaver Scientific, United Kingdom).

2.8. Measurement of reactive oxygen species (ROS)

Intracellular ROS generation was assessed using non-polar cell-permeable dye 5-(and-6)-chlromethyl-2′, 7′-dichlorodihydrofluorescein Diacetate (DCFDA) (Sigma Aldrich, USA). In brief, uninfected and virus-infected cells were harvested following respective treatments. Cells were washed to remove the remaining cell-culture media. Cells were then trypsinized followed by incubation with DCFDA (final concentration, 10 μM) for 45 min at 37 ºC in dark. Cells were then analysed directly for fluorescence emission in the FITC-channel (denoting level of ROS generation) using flow cytometry (BD FACSVerse, USA).

2.9. Statistical analysis

Statistical difference of values between two groups was estimated using Student's t-test (two-tailed). p-values were analyzed utilizing GraphPad Prism 5. Graphs provided in the figure represent data in the form of mean ± SD from three independent experiments having similar outcomes.

3. Results

3.1. SH-SY5Y infection by JEV upregulates pyruvate dehydrogenase kinase-1 abundance

To assess whether infection of SH-SY5Y cells by JEV upregulates pyruvate dehydrogenase kinase-1 (PDK-1), SH-SY5Y cells were infected with JEV at MOI: 3 for multiple time-periods as indicated in Fig. 1. SH-SY5Y cells upon infection by JEV for 48 h exhibited increase in PDK-1 abundance at protein level (modest, but statistically significant), but not following 36- or 60-hours post infection (hpi) (Fig. 1A). RNA isolated from JEV-infected SH-SY5Y (at MOI 3 and for 36-, 48- and 60-horus) cells were subjected to quantitative real-time polymerase chain reaction (qRT-PCR) for evaluating expression level of PDK-1 transcripts. qRT-PCR data also exhibited similar trend (Figure1B) as observed in Fig. 1A. Cells infected by JEV for 48-, but not 36- and 60-hours displayed upregulation of PDK-1 at transcript level. This demonstrates that JEV-induced PDK-1 upregulation in SH-SY5Y cells is a time-specific and transient event taking place at specific time-period following infection (48 h). In order to evaluate whether JEV-mediated upregulation of neuronal PDK-1 is virus-specific (i.e.: specific for JEV) or is applicable to other virus of *flavivirus* genus, we studied time-dependent expression profile of PDK-1 in SH-SY5Y cells infected with WNV (MOI: 3). However, WNV infection was not observed to upregulate PDK-1 abundance like JEV in neurons upon infection for 36-, 48- and 60-hours. Evaluation of PDK-1 protein expression level by immunoblotting experiment revealed no change in PDK-1 expression (Fig. 1C). Assessment of PDK-1 transcript abundance also presented with similar data showing no changes in PDK-1 abundance upon infection of SH-SY5Y cells by WNV for 36, 48 and 60 h (Fig. 1D).

3.2. PDK-1 upregulation promotes neuronal apoptosis in the context of infection by JEV

To check whether JEV-induced PDK-1 upregulation plays any role in virus-induced neuronal apoptosis, transient inhibition of PDK-1 utilizing endoribonuclease-prepared small interfering RNA (esiRNA) specific for human PDK-1 was employed. Transfection of JEV-infected (MOI: 3, 48 h post infection) SH-SY5Y cells with PDK-1-specific esiRNA was observed to restore JEV-mediated PDK-1 upregulation (Fig. 2A) in comparison to that of JEV-infected SH-SY5Y cells transfected with eGFP-specific esiRNA thus demonstrating specificity of PDK-1-specific esiRNA action. Restoration of virus-induced PDK-1 upregulation by PDK-1-specific esiRNA was observed to reduce cleaved caspase-9, cleaved-PARP and cleaved caspase-3 expression with respect to that in JEV-infected cells transfected with non-specific eGFP-esiRNA (Fig. 2A). Quantification of PDK-1 (Fig. 2B), cleaved caspase-9 (Fig. 2C) cleaved PARP (Fig. 2D) and cleaved caspase-3 (Fig. 2E) expression level in JEV-infected SH-SY5Y cells (from Western blotting data, Fig. 2A) upon transfection with PDK-1-specific esiRNA demonstrates reduction (albeit modest, but

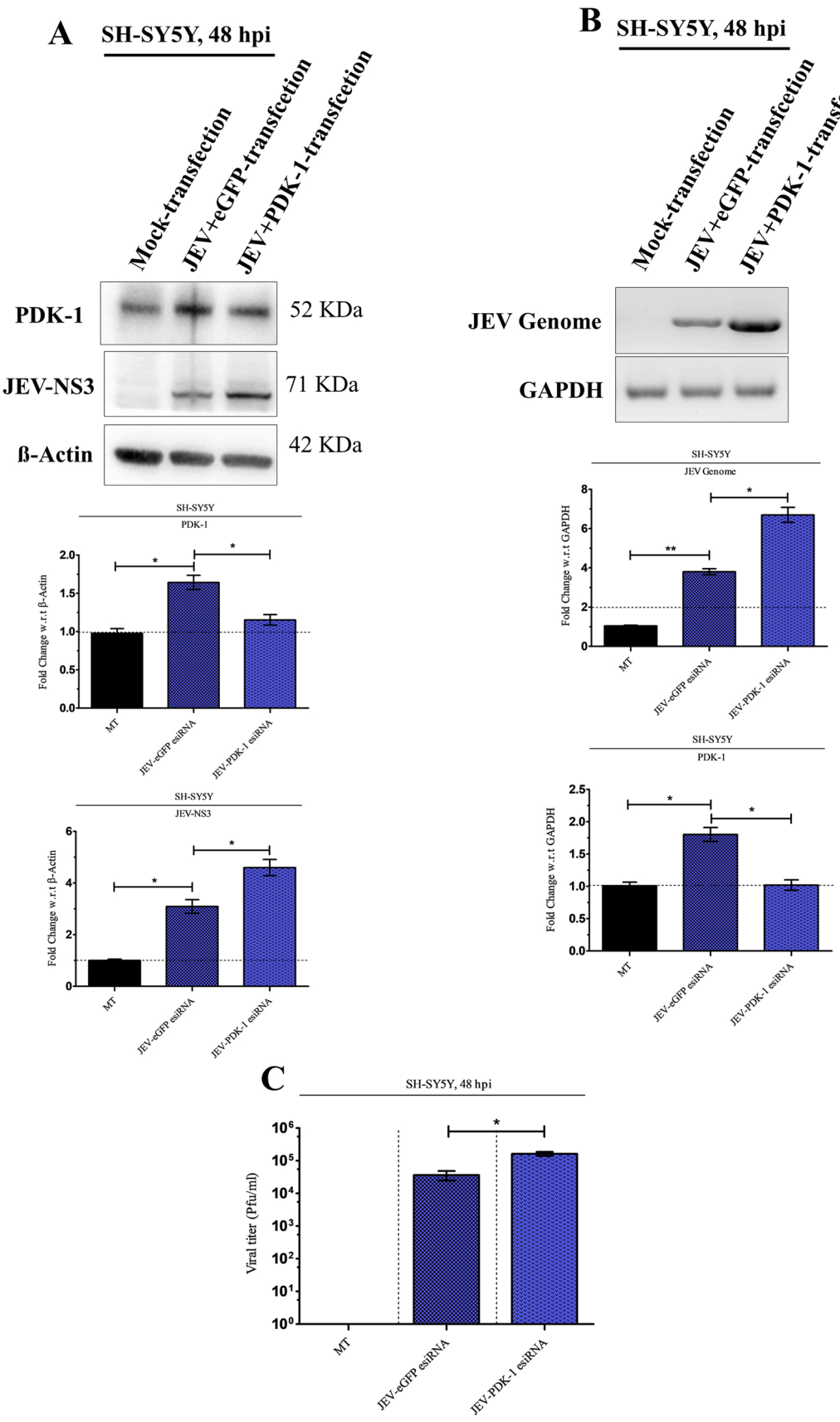

(caption on next page)

Fig. 3. PDK-1 upregulation in neuron suppresses JEV propagation. SH-SY5Y cells treated under different conditions (Uninfected + mock-transfected, JEV-infected + enhanced GFP-transfected and JEV-infected + PDK-1 esiRNA-transfected) were harvested following infection by JEV for 48 h at MOI 3. Protein isolated from the cells were subjected to immunoblotting experiment for assessing abundance of PDK1 and JEV-NS3 protein (A, quantitative analysis with respect to ß-Actin: A bottom). RNA isolated from the cells were subjected to cDNA preparation followed by qRT-PCR and semi-quantitative PCR for assessing abundance of PDK1 and JEV RNA abundance respectively (B, quantitative analysis with respect to GAPDH: B bottom). Cell-culture supernatant collected from the treated-cells mentioned above were subjected to plaque assay for determination of titer of infectious JEV particles (C). ß-Actin and GAPDH abundance was used as loading control for Western blotting and semi-quantitative/quantitative PCR experiments respectively. Data in bar graph have been presented as mean ± SD from 3 independent experiments with similar results. Statistical significance of difference in values between two groups has been evaluated using two-tailed Student's t-test. $^{**}P < 0.01$, $^{*}P < 0.05$.

statistically significant) when compared to that in infected cells transfected with eGFP-specific esiRNA. These findings hence underscore importance of JEV-induced PDK-1 upregulation in promoting neuronal apoptosis.

3.3. JEV-induced PDK-1 upregulation restricts JEV propagation in SH-SY5Y cells

In order to find out whether the observed effect of PDK-1-inhibition upon neuronal apoptosis was due to any effect of PDK-1 expression modulation upon JEV replication/propagation, JEV-NS3 abundance was assessed in JEV-infected SH-SY5Y cells transfected with eGFP-specific or PDK-1-specific esiRNA (Fig. 3A). Reversal of JEV-induced PDK-1 upregulation by transfecting SH-SY5Y cells with PDK-1-specific esiRNA was observed to result in increased JEV-NS3 protein abundance when compared to that in infected-cells transfected with eGFP-specific esiRNA (Fig. 3A). In addition to enhancing viral protein abundance, PDK-1 upregulation inhibition in the context of JEV infection displayed increased JEV-RNA in SH-SY5Y cells with respect to that in JEV-infected cells transfected with eGFP-specific esiRNA (Fig. 3B). Efficiency of PDK1-specific esiRNA in inhibiting virus-induced PDK-1 upregulation has been shown by immunoblotting (Fig. 3A) and qRT-PCR experiments (Fig. 3B) demonstrating PDK1 abundance under different experimental conditions. To conclusively establish that PDK-1-inhibiton in the face of JEV infection promotes JEV propagation in SH-SY5Y cells, titer of infectious virus particles released by cells was measured using plaque assay. PDK-1 inhibition led to increase in release of infectious JEV particles by SH-SY5Y cells than that upon transfection with eGFP-specific esiRNA (Fig. 3C). SH-SY5Y cells were infected by JEV at MOI: 3 for 48 h. The aforementioned findings thus strongly suggest role of JEV-induced PDK-1 upregulation in SH-SY5Y cells in restricting JEV propagation.

3.4. JEV-mediated PDK-1 upregulation enhances oxidative stress in SH-SY5Y cells

Report demonstrates that inhibition of PDH activity promotes development of oxidative stress (Glushakova et al., 2011) and PDK-1 is known to phosphorylate and inhibit PDH activity(Wang et al., 2021). Owing to the aforementioned facts, effect of PDK-1 upregulation in SH-SY5Y cells upon oxidative stress (in the context of JEV infection) was evaluated using 5-(and-6)-chlromethyl-2′, 7′-dichlorodihydro-fluorescein Diacetate (DCFDA). SH-SY5Y cells were transfected with eGFP-/PDK-1-specific esiRNA followed by infection with JEV (MOI: 3, 48 h). Following infection, cells undergoing different treatment conditions were collected and subjected to DCFDA staining. Reactive oxygen species (ROS) generation was analysed as histogram using flow cytometry (Fig. 4A and 4B). Relative mean fluorescence intensity (Fig. 4C) and relative median fluorescence intensity (Fig. 4D) derived from flow cytometric measurement of DCFDA staining (Fig. 4A, 4B) indicate increase in ROS synthesis by JEV-infected + EGFP-specific esiRNA-transfected cells in comparison to that in uninfected + mock-transfected cells. However, reversal of PDK-1 upregulation in SH-SY5Y cells in the setting of JEV infection by PDK-1-specific esiRNA transfection reversed JEV-induced upregulation in ROS abundance (Fig. 4C, 4D) thus concluding that PDK-1 upregulation by JEV in SH-SY5Y cells enhances oxidative stress. Since virus infection-induced generation of free radicals plays vital role in infection-associated cell death, it further strengthens our notion that PDK-1-induced oxidative stress contributes to onset of neuronal apoptosis upon infection by JEV.

4. Discussion

Albeit apoptosis is considered to be a host defense mechanism against virus infection aimed at curtailing further viral replication and release of infectious viral particles, the tissue integrity and function depends upon the cell-type undergoing apoptosis. Owing to lack of/very limited neuronal regeneration in central nervous system(Huebner and Strittmatter, 2009), loss of neurons upon JEV-induced neuroinvasion leads to severe morbidity and mortality. Flaccid paralysis of hindlimbs in murine model of JEV infection is attributed by virus-induced loss of spinal motor neurons in a cell-autonomous fashion(Bhaskar et al., 2021). Due to the robustness of network (comprising of Bcl-2 family of apoptotic proteins) activated by JEV in neurons, targeting single pro/anti-apoptotic protein to prevent activation of apoptotic machinery might be faced with limited success. It is thus imperative to decipher molecular mechanism responsible for activation of neuronal apoptosis upon JEV infection hence providing us with possible future therapeutic strategy in combating JEV infection-associated encephalitis, disease morbidity and mortality.

Recent discoveries in the field of host metabolic changes induced by virus infection have shed significant insight into how viruses hijack host metabolic pathways to meet the requirements for its own replication and propagation. Metabolic intermediates (lipid, nucleotide, carbohydrates etc.) altered following viral infection play pivotal role in promoting viral replication (Sanchez and Lagunoff, 2015). These metabolic changes mediated by virus infection might modulate the replication/propagation of the latter by multiple means. Changes in host cell metabolism might enhance supply of biomolecules necessary for viral genome replication, virus maturation in case of enveloped viruses. Modulation of metabolic pathway activity also provides virus with the energy requirements (adenosine triphosphate, ATP) required during various stages of viral life-cycle. These metabolic changes in the context of virus infection are brought about by both viral protein synthesis or by changes in host signaling pathway activity (McArdle et al., 2011). Early viral gene synthesis has been shown to enhance glycolysis upon infection by human cytomegalovirus (HCMV).

Infection by JEV results in modulation of plethora of host signaling pathways which shape the response to microbial infection. JEV infection has been observed to modulate the network of pro-/anti-apoptotic Bcl-2 protein molecules which eventually leads to disruption of mitochondria physiology thus activating apoptosome complex (Suzuki et al., 2018; Tsao et al., 2008). Multiple arms of ER stress pathway have been shown to get activated by JEV infection in neurons contributing to virus-induced cell death. Activation of PERK (Protein Kinase RNA-like ER Kinase)-CHOP (C/EBP Homologous protein) axis results in activation of apoptotic machinery thus culminating into neuronal death (Wang et al., 2019). Activation of JNK pathway has also been shown to play a pivotal role in inducing activation of intrinsic apoptotic pathway thus leading to cellular demise (Huang et al., 2016). JNK promotes apoptosis by multiple means which include regulation of transcription of anti-/pro-apoptotic molecules thus changing their relative abundance, inciting mitochondrial damage (Dhanasekaran and Reddy, 2008) etc. Interestingly, JNK has also been reported to negatively regulate the

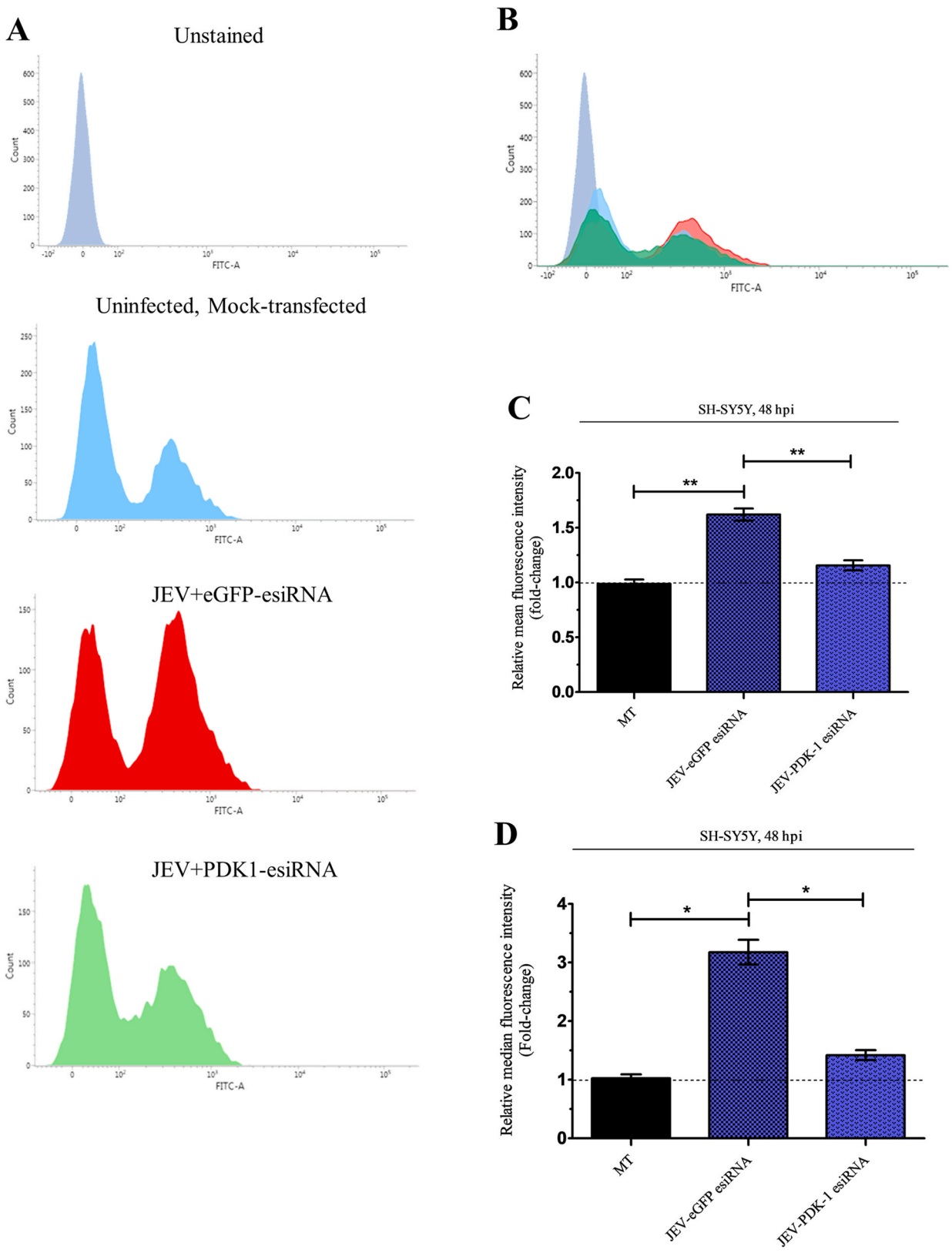

Fig. 4. JEV-induced PDK-1 upregulation promotes reactive oxygen species generation in SH-SY5Y cells. Histogram showing ROS generation by SH-SY5Y cells treated under variable conditions as represented in figure (A) (unstained + uninfected, DCFDA-Stained + uninfected + mock-transfected, DCFDA-stained + JEV-infected + enhanced GFP-transfected, DCFDA-stained + JEV-infected + PDK-1 esiRNA-transfected) and harvested after JEV infection for 48 h at 3 MOI. (B) Overlap of histograms shown in A denoting difference in ROS abundance in SH-SY5Y cells treated under different conditions. Relative mean fluorescence intensity (C) and relative median fluorescence intensity (D) of SH-SY5Y cells uninfected/JEV-infected + mock-transfected/enhanced GFP-transfected/PDK-1 esiRNA-transfected (infection performed at MOI 3 and for 48 h) have been derived from histograms. Bar graphs shown in the figure represent data in the form of mean ± SD from three different experiments. Two-tailed Student's t-test has been used for estimation of statistical difference of values between two groups. $^{**}P < 0.01$, $^{*}P < 0.05$.

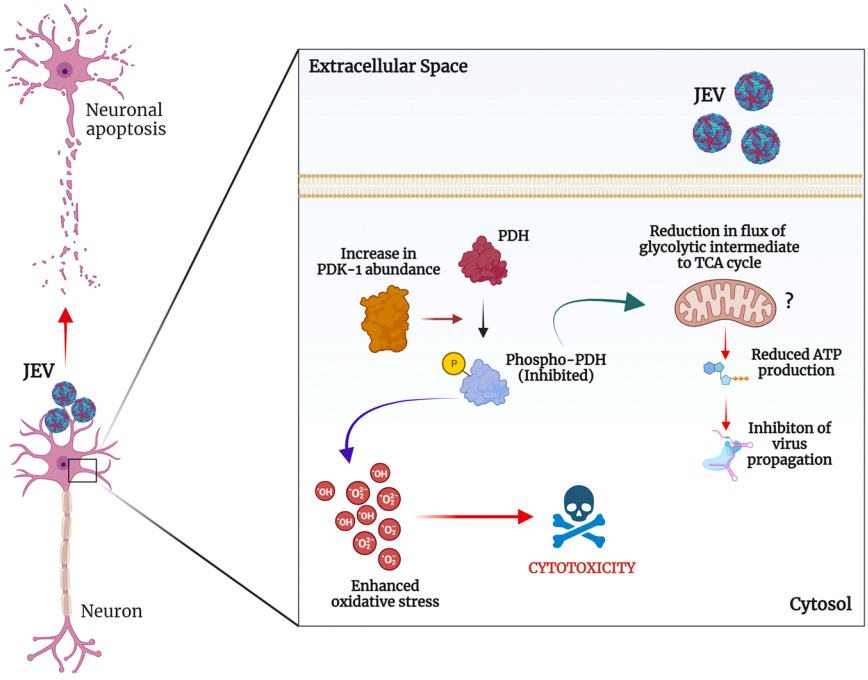

Fig. 5. Schematic diagram representing mechanistic basis for PDK-1′s role in promoting neuronal apoptosis upon JEV infection. JEV-induced PDK-1 upregulation in neurons promotes oxidative stress which exerts deleterious effects upon cellular physiology culminating into neuronal apoptosis. PDK-1 upregulation-induced inhibition of PDH activity might result in reduced ATP generation by reducing flux of metabolic intermediates from glycolysis to TCA cycle, which might explain the restrictive effect of increased PDK-1 abundance upon JEV propagation.

activity of PDH complex (Zhou et al., 2009) thus reducing the flux of metabolite from glycolysis to TCA cycle in a pyruvate dehydrogenase kinase-dependent fashion. Although activated-JNK has been demonstrated to physically interact with mitochondria, it is not capable of translocating into mitochondrial matrix which hosts the PDH-complex. Owing to the aforementioned fact, JNK activation was hypothesized to activate downstream signaling which eventually results in PDH phosphorylation and inhibition. PDH-complex subunit acts as a primary substrate for PDK enzyme which phosphorylates the former leading to PDH activity inhibition. Indeed, activation of JNK in neuronal cells has been reported to inhibit PDH activity in PDK-dependent manner (Zhou et al., 2009). In light of aforementioned findings, and given the importance of changes in glucose metabolism and its effect upon viral replication/propagation, we were interested to study whether JEV infection regulates abundance of PDK-1 enzyme (which has been reported to phosphorylate PDH subunit followed by inhibition of the latter).

In this study, we have demonstrated that human neuronal cell-line upon infection by JEV exhibits upregulation of PDK-1 abundance. In order to assess whether JEV-induced PDK-1 upregulation in neurons is a virus-specific event or can be applied to other virus of *flavivirus* genus, PDK-1 expression level was estimated in human neuronal cell-line infected with West Nile Virus (WNV). WNV like JEV, is a positive-sense single-stranded RNA virus belonging to family *Flaviviridae* (Suthar et al., 2013). WNV upon infecting human neuronal cell-line however was not observed to upregulate PDK-1 abundance thus pointing JEV-mediated PDK-1 upregulation as a virus-specific event. Inhibition of JEV-induced PDK-1 upregulation was demonstrated to inhibit neuronal apoptosis. Effect of PDK-1 inhibition upon JEV propagation was studied to check whether PDK-1 inhibition-associated reduction is neuronal apoptosis is due to any inhibition of JEV propagation. Surprisingly, inhibition of PDK-1 was associated with increase in magnitude of viral protein and RNA abundance. Release of infectious JEV particles was also observed to increase upon PDK-1 inhibition in the context of JEV infection. Although the aforementioned findings related to enhanced JEV propagation upon PDK-1 inhibition contradict PDK-1′s effect upon neuronal apoptosis, one possible explanation might be that the magnitude of increase in JEV propagation is not sufficient enough to counteract any other protective mechanism set into action by PDK-1 inhibition thus leading to reduction in neuronal apoptosis. PDK-1 phosphorylates and thus inhibits PDH activity, which results in reduction in TCA cycle activity. In addition to that, lack of any increase in glycolytic activity, as indicated by no alteration in hexokinase-2 transcript level upon JEV infection (Supplementary Figure 1), denotes reduction in ATP generation. HCMV replication has been shown to be negatively regulated upon depletion of intracellular ATP (Chambers et al., 2010). PDK-1 upregulation resulting into inhibition of PDH activity might thus lead to reduction in ATP hence negatively controlling JEV replication. PDK-1 inhibition on the other hand thus can result in disinhibition of PDH activity leading to restoration of ATP levels which can explain the ensuing increase in JEV propagation. Report indicates role of PDH inhibition in increased accumulation of ROS (Glushakova et al., 2011). ROS accumulation has been demonstrated to play crucial role in virus-induced cell death (Zhang et al., 2019). Outcome of Dengue virus infection in patients has been shown to depend upon magnitude of ROS generation. Highest levels of oxidative stress upon Dengue virus infection in patients can be observed upon Dengue shock-syndrome, followed by Dengue hemorrhagic fever and dengue fever. This positive correlation is thus suggestive of role of oxidative stress in Dengue infection pathogenesis. ROS generation in monocyte-derived macrophages upon Dengue infection has been shown to modulate innate immunity and apoptosis. ROS generation in the context of JEV infection has been reported to play role in promoting cellular apoptosis. HCV infection has been shown to elicit upregulation in ROS generation by negatively effecting mitochondrial physiology. Free radicals generated in response to HCV infection has been linked to DNA damage thus culminating into viral disease pathology. ROS-mediated peroxidation of intracellular membrane lipid thus might interfere negatively with organelle physiology resulting into apoptosis. Increase in PDK-1 expression level hence might lead to enhanced generation of ROS in a PDH-dependent fashion thus leading to neuronal death. Indeed, our study shows JEV infection of SH-SY5Y cells was accompanied by increase in oxidative stress which was found to be ameliorated upon reversal of JEV-induced PDK-1 upregulation. The stated evidences thus substantiate our conclusion that JEV-mediated PDK-1 upregulation in human neuronal cell-line promotes apoptosis in an oxidative stress-dependent fashion.

In summary (Fig. 5), in our present study we have demonstrated that JEV upon infecting neuronal cells upregulate PDK-1 abundance.

Although inhibition of PDK-1 upregulation was seen to be associated with increase in JEV propagation, JEV-induced neuronal apoptosis was observed to be downregulated upon PDK-1 inhibition. Negatively interfering with PDK-1 expression in the context of JEV infection was found to reduce JEV-induced ROS generation thus leading to less cell death. These findings thus point towards interaction between factors like ROS-induced cellular damage and level of viral replication in finally deciding neuronal fate (in terms of apoptosis) upon JEV infection.

CRediT authorship contribution statement

Surajit Chakraborty: Conceptualization, methodology, validation, data curation, Roles/Writing- original draft. Ellora Sen: Conceptualization, funding acquisition, Writing: review & editing. **Anirban Basu:** Conceptualization, funding acquisition, supervision, Writing: review & editing.

Conflict of interest

Authors declare no conflict of interest.

Acknowledgments

The current study has been supported by J C Bose Fellowship (JCB/2020/000037) to AB and SERB Power Fellowship (SPF/2021/000199) to ES from the Science and Engineering Research Board, Ministry of Science and Technology, Government of India. We acknowledge Manish Kumar Dogra and Dr. Kanhaiya Lal Kumawat for their technical assistance. The schematic diagram has been prepared using BioRender.

References

Bhaskar, M., Mukherjee, S., Basu, A., 2021. Involvement of RIG-I pathway in neurotropic virus-induced acute flaccid paralysis and subsequent spinal motor neuron death. https://doi.org/10.1128/mBio.

Bhatt, A.N., Kumar, A., Rai, Y., Kumari, N., Vedagiri, D., Harshan, K.H., Chinnadurai, V., Chandna, S., 2022. Glycolytic inhibitor 2-deoxy-D-glucose attenuates SARS-CoV-2 multiplication in host cells and weakens the infective potential of progeny virions. Life Sci. 295 https://doi.org/10.1016/j.lfs.2022.120411.

Chakraborty, S., Basu, A., 2022. miR-451a regulates neuronal apoptosis by modulating 14-3-3ζ-JNK axis upon flaviviral infection. mSphere. https://doi.org/10.1128/msphere.00208-22.

Chambers, J.W., Maguire, T.G., Alwine, J.C., 2010. Glutamine metabolism is essential for human cytomegalovirus infection. J. Virol. 84, 1867–1873. https://doi.org/10.1128/jvi.02123-09.

Chambers, T.J., Diamond, M.S., 2003. Pathogenesis of flavivirus encephalitis.

Dhanasekaran, D.N., Reddy, E.P., 2008. JNK signaling in apoptosis. Oncogene. https://doi.org/10.1038/onc.2008.301.

Fontaine, K.A., Sanchez, E.L., Camarda, R., Lagunoff, M., 2015. Dengue virus induces and requires glycolysis for optimal replication. J. Virol. 89, 2358–2366. https://doi.org/10.1128/jvi.02309-14.

Glushakova, L.G., Judge, S., Cruz, A., Pourang, D., Mathews, C.E., Stacpoole, P.W., 2011. Increased superoxide accumulation in pyruvate dehydrogenase complex deficient fibroblasts. Mol. Genet. Metab. 104, 255–260. https://doi.org/10.1016/j.ymgme.2011.07.023.

Huang, M., Xu, A., Wu, X., Zhang, Y., Guo, Y., Guo, F., Pan, Z., Kong, L., 2016. Japanese encephalitis virus induces apoptosis by the IRE1/JNK pathway of ER stress response in BHK-21 cells. Arch. Virol. 161, 699–703. https://doi.org/10.1007/s00705-015-2715-5.

Huebner, E.A., Strittmatter, S.M., 2009. Axon regeneration in the peripheral and central nervous systems. Results Probl. Cell Differ. 48, 339–351. https://doi.org/10.1007/400_2009_19.

Johnson, R.T., Burke, D.S., Elwell, M., Leake, C.J., Nisalak, A., Hoke, C.H., Lorsomrudee, W., 1985. Japanese encephalitis: immunocytochemical studies of viral antigen and Inflammatory cells in fatal cases. Ann. Neurol. 18, 567–573. https://doi.org/10.1002/ana.410180510.

Leier, H.C., Messer, W.B., Tafesse, F.G., 2018. Lipids and pathogenic flaviviruses: an intimate union. PLOS Pathog. 14. https://doi.org/10.1371/journal.ppat.1006952.

McArdle, J., Schafer, X.L., Munger, J., 2011. Inhibition of calmodulin-dependent kinase kinase blocks human cytomegalovirus-induced glycolytic activation and severely attenuates production of viral progeny. J. Virol. 85, 705–714. https://doi.org/10.1128/jvi.01557-10.

Medigeshi, G.R., Lancaster, A.M., Hirsch, A.J., Briese, T., Lipkin, W.I., DeFilippis, V., Früh, K., Mason, P.W., Nikolich-Zugich, J., Nelson, J.A., 2007. West Nile virus infection activates the unfolded protein response, leading to CHOP induction and apoptosis. J. Virol. 81, 10849–10860. https://doi.org/10.1128/jvi.01151-07.

Neufeldt, C.J., Cortese, M., Acosta, E.G., Bartenschlager, R., 2018. Rewiring cellular networks by members of the Flaviviridae family. Nat. Rev. Microbiol. https://doi.org/10.1038/nrmicro.2017.170.

Rothan, H.A., Fang, S., Mahesh, M., Byrareddy, S.N., 2019. Zika virus and the metabolism of neuronal cells. Mol. Neurobiol. https://doi.org/10.1007/s12035-018-1263-x.

Sanchez, E.L., Lagunoff, M., 2015. Viral activation of cellular metabolism. Virology. https://doi.org/10.1016/j.virol.2015.02.038.

Saw, K., Myint, A., Raengsakulrach, B., Young, G.D., Gettayacamin, M., Ferguson, L.M., Innis, B.L., Hoke, C.H., Vaughn, D.W., 1999. Production of lethal infection that resembles fatal human disease by intranasal inoculation of macaques with Japanese encephalitis virus. Am. J. Trop. Med. Hyg.

Solomon, T., Dung, N.M., Kneen, R., Gainsborough, M., Vaughn, D.W., Khanh, V.T., 2000. Japanese encephalitis. J. Neurol. Neurosurg. Psychiatry. https://doi.org/10.1136/jnnp.68.4.405.

Suthar, M.S., Diamond, M.S., Gale, M., 2013. West Nile virus infection and immunity. Nat. Rev. Microbiol. https://doi.org/10.1038/nrmicro2950.

Suzuki, T., Okamoto, T., Katoh, H., Sugiyama, Y., Kusakabe, S., Tokunaga, M., Hirano, J., Miyata, Y., Fukuhara, T., Ikawa, M., Satoh, T., Yoshio, S., Suzuki, R., Saijo, M., Huang, D.C.S., Kanto, T., Akira, S., Matsuura, Y., 2018. Infection with flaviviruses requires BCLXL for cell survival. PLOS Pathog. 14 https://doi.org/10.1371/journal.ppat.1007299.

Tsao, C.H., Su, H.L., Lin, Y.L., Yu, H.P., Kuo, S.M., Shen, C.I., Chen, C.W., Liao, C.L., 2008. Japanese encephalitis virus infection activates caspase-8 and -9 in a FADD-independent and mitochondrion-dependent manner. J. Gen. Virol. 89, 1930–1941. https://doi.org/10.1099/vir.0.2008/000182-0.

Turtle, L., Solomon, T., 2018. Japanese encephalitis-the prospects for new treatments. Nat. Rev. Neurol. https://doi.org/10.1038/nrneurol.2018.30.

Wang, Q., Xin, X., Wang, T., Wan, J., Ou, Y., Yang, Z., Yu, Q., Zhu, L., Guo, Y., Wu, Y., Ding, Z., Zhang, Y., Pan, Z., Tang, Y., Li, S., Kong, L., 2019. Japanese encephalitis virus induces apoptosis and encephalitis by activating the PERK pathway. J. Virol. 93 https://doi.org/10.1128/jvi.00887-19.

Wang, X., Shen, X., Yan, Y., Li, H., 2021. Pyruvate dehydrogenase kinases (PDKs): an overview toward clinical applications. Biosci. Rep. https://doi.org/10.1042/BSR20204402.

Zhang, Z., Rong, L., Li, Y.P., 2019. Flaviviridae viruses and oxidative stress: implications for viral pathogenesis. Oxid. Med. Cell. Longev. https://doi.org/10.1155/2019/1409582.

Zhou, Q., Lam, P.Y., Han, D., Cadenas, E., 2009. Activation of c-Jun-N-terminal kinase and decline of mitochondrial pyruvate dehydrogenase activity during brain aging. FEBS Lett. 583, 1132–1140. https://doi.org/10.1016/j.febslet.2009.02.043.